



**Landslide inventory
development in a
data sparse region**

J. C. Robbins and
M. G. Petterson

This discussion paper is/has been under review for the journal Natural Hazards and Earth System Sciences (NHESS). Please refer to the corresponding final paper in NHESS if available.

Landslide inventory development in a data sparse region: spatial and temporal characteristics of landslides in Papua New Guinea

J. C. Robbins¹ and M. G. Petterson²

¹Met Office, Fitzroy Road, Exeter, Devon, UK

²Secretariat of the Pacific Community, Suva, Fiji

Received: 15 July 2015 – Accepted: 16 July 2015 – Published: 17 August 2015

Correspondence to: J. C. Robbins (joanne.robbs@metoffice.gov.uk)

Published by Copernicus Publications on behalf of the European Geosciences Union.

[Title Page](#)

[Abstract](#)

[Introduction](#)

[Conclusions](#)

[References](#)

[Tables](#)

[Figures](#)

[⏪](#)

[⏩](#)

[◀](#)

[▶](#)

[Back](#)

[Close](#)

[Full Screen / Esc](#)

[Printer-friendly Version](#)

[Interactive Discussion](#)



Abstract

In Papua New Guinea (PNG) earthquakes and rainfall events form the dominant trigger mechanisms capable of generating many landslides. Large volume and high density landsliding can result in significant socio-economic impacts, which are felt particularly strongly in the largely subsistence-orientated communities which reside in the most susceptible areas of the country. As PNG has undergone rapid development and increased external investment from mining and other companies, population and settled areas have increased, hence the potential for damage from landslides has also increased. Information on the spatial and temporal distribution of landslides, at a regional-scale, is critical for developing landslide hazard maps and for planning, sustainable development and decision making. This study describes the methods used to produce the first, country-wide landslide inventory for PNG and analyses of landslide events which occurred between 1970 and 2013. The findings illustrate that there is a strong climatic control on landslide-triggering events and that the majority (~ 61 %) of landslides in the PNG landslide inventory are initiated by rainfall related triggers. There is also large year to year variability in the annual occurrence of landslide events and this is related to the phase of El Niño Southern Oscillation (ENSO) and mesoscale rainfall variability. Landslide-triggering events occur during the north-westerly monsoon season during all phases of ENSO, but less landslide-triggering events are observed during drier season months (May to October) during El Niño phases, than either La Niña or ENSO neutral periods. This analysis has identified landslide hazard hotspots and relationships between landslide occurrence and rainfall climatology and this information can prove to be very valuable in the assessment of trends and future behaviour, which can be useful for policy makers and planners.

Landslide inventory development in a data sparse region

J. C. Robbins and
M. G. Petterson

[Title Page](#)

[Abstract](#)

[Introduction](#)

[Conclusions](#)

[References](#)

[Tables](#)

[Figures](#)

[⏪](#)

[⏩](#)

[◀](#)

[▶](#)

[Back](#)

[Close](#)

[Full Screen / Esc](#)

[Printer-friendly Version](#)

[Interactive Discussion](#)



1 Introduction

Papua New Guinea (PNG) is particularly prone to landslides due its geomorphology, climate and geology. In recent years there have been numerous landslides which have resulted in large numbers of fatalities and caused significant socio-economic impacts upon communities surrounding the landslide site and further afield (e.g. Tumbi Landslide in Southern Highlands Province; Robbins et al., 2013). Although PNG has experienced some of largest recorded landslides in the world (e.g. Kaiapit Landslide in 1988, Peart, 1991a; Drechsler et al., 1989, and the Bairaman Landslide in 1985, King and Loveday, 1985), research has tended to focus on basin scale landsliding and has largely involved documenting the characteristics of individual landslides or a cluster of landslides associated with a specific trigger mechanism (Greenbaum et al., 1995). There have been field investigations to map landslide scars in particularly sensitive regions of the country, such as along the Highlands Highway (Tutton and Kuna, 1995; Kuna, 1998) and in close proximity to mining operations (Hearn, 1995; Fookes et al., 1991), but these studies have remained largely isolated and do not conform to a standard of landslide recording. To understand the temporal and spatial characteristics of landslides and their trigger mechanisms, assessments at a regional-scale are required, particularly when trying to determine trends or develop models. Development of such regional-scale inventories can prove challenging particularly in a region such as PNG, as the nature of landslides means that: (1) they frequently result in impacts over small areas compared to impacts associated with larger-scale natural hazards and (2) the areas affected by landslides are often remote and difficult to access, as well as being widely distributed relative to one another (Kirschbaum et al., 2009; Petley, 2012). Therefore, although there have been a number of fieldwork campaigns to update and extend existing geological maps in PNG, the development of regional landslide hazard maps, based on fieldwork, has proven difficult. By extension, this has limited the development of landslide inventories in the region. The aim of this study is to build-upon existing methods and approaches (Greenbaum et al., 1995; Blong, 1985) to construct

Landslide inventory development in a data sparse region

J. C. Robbins and
M. G. Petterson

[Title Page](#)

[Abstract](#)

[Introduction](#)

[Conclusions](#)

[References](#)

[Tables](#)

[Figures](#)

[⏪](#)

[⏩](#)

[◀](#)

[▶](#)

[Back](#)

[Close](#)

[Full Screen / Esc](#)

[Printer-friendly Version](#)

[Interactive Discussion](#)



ment of material is generally limited, while events occurring on steeper slopes ($> 30^\circ$) can result in deposits with volumes in excess of $500\,000\text{ m}^3$ (e.g. Dinidam Landslide; Blong, 1986). Numerous slumps, of varying size, have been observed along the Highlands Highway (Tutton and Kuna, 1995; Kuna, 1998) and can regularly lead to road closures and property damage. In addition to slumps, mudslides also result in damage and disruption, affecting both infrastructure and property, along the Highlands Highway. Defined as “masses of argillaceous, silty or very fine sandy debris” which displace material by “sliding on discrete boundary surfaces in relatively slow moving lobate forms” (Stead, 1990), they are most frequently observed in areas which are underlain by the Chim Formation. Movements of this type are particularly problematic because their generally slow displacement rate ($\sim 60\text{ mm yr}^{-1}$ at Yakatabari; Blong, 1985) can increase rapidly associated with localized changes in shear strength and pore water pressure. Furthermore variations in depth, width and style of movement (Comegna et al., 2007) and the fact that they can occur on very low slope angles (between 6 and 15°), which coincide with settled and populated areas, means that they are difficult to mitigate against. By contrast, translational slides and rockslides typically occur on very steep slopes (between 30 and 50°) in areas with deeply incised terrain. The failure mechanisms of these slides are strongly influenced by bedding planes, joints, faults and the interface between weathered material and fresh bedrock. Given the highly fractured and deformed nature of many rocks in PNG these slides can occur in a wide range of geological materials. However, the distribution of translational slides and rockslides is strongly linked to the topography, making areas susceptible to them easier to identify.

Landslide inventory development in a data sparse region

J. C. Robbins and
M. G. Petterson

[Title Page](#)[Abstract](#)[Introduction](#)[Conclusions](#)[References](#)[Tables](#)[Figures](#)[⏪](#)[⏩](#)[◀](#)[▶](#)[Back](#)[Close](#)[Full Screen / Esc](#)[Printer-friendly Version](#)[Interactive Discussion](#)

2 Materials and methods

2.1 Regional landslide inventory construction: criteria, sources and structure

PNG currently has no systematic, routine approach for recording landslide events. This means that although a large number of landslides have been identified by their scars and deposits (Kuna, 1998) the dates of events are rarely recorded. To collate a landslide inventory which can be used to examine the temporal and spatial frequency of landslides and the corresponding relationship between these events and potential landslide triggers, it is essential that the dates and locations of landslides are recorded. Therefore, in the new PNG inventory only those landslides where both the date and location could be established with reasonable accuracy were entered. The precise date of landslide occurrence is often difficult to determine, however, where there are eye witnesses to the event the day of initiation can be recorded. In instances with no eye witnesses to the event, the time of initiation was approximated using a minimum and a maximum date boundary relating to the earliest and latest dates within which the landslide event occurred. The minimum and maximum dates frequently related to the start and end dates of potential landslide-triggering events, such as a flood event, which resulted in landslides. The basic location information required for a landslide to be included in the inventory was either a village or landmark name and the administrative province. All landslide records were analysed closely for the veracity and accuracy of essential data in terms of geographical locality, time, corroborating evidence (e.g. witness statements, press, quality of writing and reporting), and incident impact. Many records were dismissed as they “failed” the quality test needed for a study such as this.

Records of landslide activity were collected from a number of sources, including:

- technical reports and site inspection logs obtained from the PNG Mineral Resources Authority (MRA) and the Department of Mineral Policy and Geohazards Management archives;
- accessible journal publications;

Landslide inventory development in a data sparse region

J. C. Robbins and
M. G. Petterson

[Title Page](#)

[Abstract](#)

[Introduction](#)

[Conclusions](#)

[References](#)

[Tables](#)

[Figures](#)

[⏪](#)

[⏩](#)

[◀](#)

[▶](#)

[Back](#)

[Close](#)

[Full Screen / Esc](#)

[Printer-friendly Version](#)

[Interactive Discussion](#)



- newspaper/media records;
- internet publications (e.g. Office for the Coordination of Humanitarian Affairs (OCHA)/ReliefWeb);
- supplementary hazard and disaster archives – e.g. Dartmouth Flood Observatory (Brackenridge, 2010; Brackenridge and Karnes, 1996); USGS National Earthquake Information Centre (NEIC); OFDA/CRED International Disaster Database (EM-DAT, Guha-Sapir and Below, 2002); Global Disaster Identifier Number (GLIDE).

Each data source used to construct the new landslide inventory had its own uncertainties and limitations and therefore the details captured for each landslide entry vary in completeness and scientific content. The most consistently available data for a landslide event were the (approximate) date of occurrence, affected areas, trigger mechanism (i.e., heavy rainfall) and the impacts of the event. Less consistently reported were the landslide type and the landslide size (volume and/or area affected). A full list of the critical and relevant information collected for each landslide entry, are shown in Table 1.

The development of a landslide database has a number of complexities. Firstly, although the majority of information sources documented individual landslides which could be spatially and temporally identified, there were a number of occasions when terms such as “some” or “numerous” were used to describe a landslide cluster, with no further spatial or temporal information related to the individual landslide deposits. In these instances, the sources often outlined the area or villages affected by the landslides but did not provide an indication of the exact number of landslides which had contributed to the observed impacts. To account for this, an additional attribute column referred to as “landslide cluster group size” was added to the database. This allowed each entry to be assigned to one of the four cluster group sizes, representing the number of landslides that were believed to have been associated with the database entry: (1) 1–10, (2) 10–100, (3) 100–1000 or (4) > 1000. Where sources indicated that landslides affected multiple villages, resulting from the same potential triggering factors,

Landslide inventory development in a data sparse region

J. C. Robbins and
M. G. Petterson

[Title Page](#)

[Abstract](#)

[Introduction](#)

[Conclusions](#)

[References](#)

[Tables](#)

[Figures](#)



[Back](#)

[Close](#)

[Full Screen / Esc](#)

[Printer-friendly Version](#)

[Interactive Discussion](#)



an entry for each unique spatial location affected was included in the database. This method aims to capture some of the uncertainty around the recording of the “true” number of landslides initiated by a triggering event, while maintaining the integrity of those events which have the required temporal and spatial information necessary for analysing patterns, trends and triggering mechanisms.

Secondly, the data sources used to collate the PNG inventory are produced by a range of authors (e.g. research scientists, geologists, media correspondents and humanitarian agencies), some of whom have no specialist knowledge of documenting landslide events. This introduces inaccuracies particularly with regard to the more technical language used to document the event, such as identifying landslide type. In media publications for example, the majority of events are described using the term “landslide”. In a small number of cases however, the landslides are referred to as mudflows but there is little evidence to suggest that this term reflects the Cruden and Varnes (1996) landslide classification. It should also be noted that there are potential inaccuracies where landslide triggers have been pre-determined in the media and other information sources, without a site inspection of the landslide by geotechnical specialists. In many instances the decision on which type of triggering event led to a landslide is based on the testimonies of people living within the affected community. The decision was taken to include information related to the potential trigger if it was available, regardless of the data source, as in the majority of cases the triggering events could be cross-referenced and verified, in terms of their timing and location by using multiple hazard and disaster databases. This approach meant that it was possible to provide corroborating support as to whether earthquakes, flooding or tropical cyclones could have contributed to the landslide entries recorded. Furthermore, it allowed multiple potential triggering factors to be attributed to a single database entry if the need was required. Data for other attributes, such as landslide type and size were only added where information was available from a scientific source (e.g. technical site reports or journal publications).

Landslide inventory development in a data sparse region

J. C. Robbins and
M. G. Petterson

[Title Page](#)

[Abstract](#)

[Introduction](#)

[Conclusions](#)

[References](#)

[Tables](#)

[Figures](#)



[Back](#)

[Close](#)

[Full Screen / Esc](#)

[Printer-friendly Version](#)

[Interactive Discussion](#)



Landslide inventory development in a data sparse region

J. C. Robbins and
M. G. Petterson

[Title Page](#)

[Abstract](#)

[Introduction](#)

[Conclusions](#)

[References](#)

[Tables](#)

[Figures](#)

[⏪](#)

[⏩](#)

[◀](#)

[▶](#)

[Back](#)

[Close](#)

[Full Screen / Esc](#)

[Printer-friendly Version](#)

[Interactive Discussion](#)



tones), which become exposed following landslides, can be differentiated from vegetated slopes (variations of red tones). FCC images were then overlain on digital terrain and settlement data so that the location and, where possible, size of the landslide(s) could be verified (Fig. 3). In order to confirm that the blue tones observed in the FCC images were associated with landslide scars, the Digital Number (DN) values of the 7 bands were extracted from the area identified as a landslide scar and compared against the typical spectral ranges indicative of many active landslides (Table 2; Petley, 2002). If the values corresponded well, then the landslide entry was considered spatially verified. Although this method proved useful for a number of the landslide entries, cloud cover and shadowing prevented other landslide entries being verified with this technique. Furthermore landslides with widths or lengths smaller than 50 m could not be captured, due to the resolution of Landsat images (Petley, 2002).

Quantifying spatial uncertainty is particularly challenging where a wide variety of data sources have been used to collate the landslide inventory, as in this case. Therefore in this study, each entry is assigned to a spatial uncertainty group based on a more subjective decision framework. The “low uncertainty” group represents entries which were digitized based on information from journal publications and/or site inspection reports and the satellite-based FCC method. Other entries included in this group, were those where latitude and longitude information of the landslide site (i.e. the location of the landslide deposit) were available. The “medium uncertainty” group represents entries where the village or landmark affected was identified and successfully cross-referenced with MRA settlement data so that a latitude and longitude for the affected site(s) was identified. The “high uncertainty” group represents entries where only an approximate area, such as the river catchment or Local Level Government (LLG) area could be identified. In these instances an approximate latitude and longitude point representative of the catchment or LLG area were recorded in the database. In the case of earthquake-induced landsliding, where information on the location of landslides was scarce, the earthquake epicentre or a point representative of the area of high den-

sity landsliding was recorded. In both cases these entries were assigned to the “high uncertainty” group.

In addition to spatial uncertainty, the availability of temporal information varied significantly depending on the data source used to identify the landslide. For very large or high-density landslides which resulted in large socio-economic impacts, the dates when landslides occurred were often clearly recorded in either site inspection reports or scientific journal publications. However where landslides were identified as a secondary natural hazard, occurring as a result of flooding or an earthquake, the dates of associated landslides were poorly recorded. In these instances, landslide initiation dates could only be estimated based on the date of the earthquake or the period over which flooding was recorded. For these events, the estimated time of landslide initiation was constrained between a minimum and maximum date boundary. This was accomplished by cross-referencing the date and potential landslide trigger against multiple hazard and disaster databases. For flood induced landslides, the Dartmouth Flood Observatory archive (Brakenridge, 2010) was particularly useful, as it compiles flood inundation extents and additional impact information, including secondary hazards such as landslides. This information has been collected since 1985 using news, governmental, instrumental and remote sensing sources. For earthquake-induced landslides, the PNG Geophysical Observatory and the USGS PAGER (Prompt Assessment of Global Earthquakes for Response) databases were used. Using information from the multiple hazard and disaster databases two distinct fields were added to the inventory: a start and end date boundary, holding information on the day, month and year in each case, relating to the earliest and latest possible date, respectively, when landslides could have been initiated. By carefully cross-referencing each landslide entry, the uncertainty around the time and duration of each potential triggering-event was reduced. For 80 % of entries, the time over which landslides were likely to have been initiation could be constrained within a period of 10 days or less. For the remaining 20 % of entries, triggering event durations exceeded 10 days. For 9 % of those entries, the duration of

Landslide inventory development in a data sparse region

J. C. Robbins and
M. G. Petterson

[Title Page](#)

[Abstract](#)

[Introduction](#)

[Conclusions](#)

[References](#)

[Tables](#)

[Figures](#)

[⏪](#)

[⏩](#)

[◀](#)

[▶](#)

[Back](#)

[Close](#)

[Full Screen / Esc](#)

[Printer-friendly Version](#)

[Interactive Discussion](#)



precipitation (MAP) and 3-monthly seasonal mean precipitation maps, as calculated from monthly data over the 1970–2010 reference period, have also been produced so that rainfall distributions can be reviewed relative to landslide affected locations.

3 Results

3.1 Landslide inventory statistics

The database consists of 167 entries recorded between January 1970 and December 2013. Each entry represents a single landslide occurrence or a cluster of landslides, identifiable by a unique spatial location. The spatial locations of individual landslides or clusters of landslides are provided by latitude and longitude points, which are additionally assigned to a spatial uncertainty group (low, medium and high). The majority (~ 63 %) of entries are in the medium spatial uncertainty group, representing entries where latitude and longitude information for the affected village or landmark associated with the landslide(s) has been successfully cross-referenced with MRA settlement data. In these instances, the landslide or landslide cluster is expected to be within 10 km of the village/landmark identified in the source material. Approximately 10 and 26 % of entries fall into the high uncertainty and low uncertainty groups, respectively. The landslides collected in the database tend to represent large-scale, high-to medium-impact events. The magnitude of the landslide events has been assessed predominantly on the impacts the event had upon the community, as this information was more readily available than quantitative size (volume or area) information. 61 % of entries had impact information available for analysis and 38 % of these can be categorized as high-impact landslide events which resulted in fatalities and additional damage to infrastructure. Medium impact landslides, representing those where there was significant damage affecting a number of different types of infrastructure but no recorded fatalities account for 43 % of the entries where this information was available, while 19 % of entries can be categorised as low impact landslides which resulted in some minor

Landslide inventory development in a data sparse region

J. C. Robbins and
M. G. Petterson

[Title Page](#)

[Abstract](#)

[Introduction](#)

[Conclusions](#)

[References](#)

[Tables](#)

[Figures](#)



[Back](#)

[Close](#)

[Full Screen / Esc](#)

[Printer-friendly Version](#)

[Interactive Discussion](#)



and Nieuwolt, 1998). Using the NOAA/ESRL/PSD bimonthly, ranked index of the Multivariate ENSO Index (MEI; Wolter and Timlin, 1993, 1998), years associated with the extreme modes of the southern oscillation have been identified. Based on these data, collected in 2012, Table 4 illustrates years which are associated with El Niño events and La Niña events, respectively. It is widely acknowledged that El Niño introduces “typically” drier than normal conditions to PNG (McVicar and Bierwirth, 2001) as the zone of deep convection, associated with the rising limb of the Walker Circulation, accompanies the eastward propagation of warmer sea surface temperatures (Qian et al., 2010), and that La Niña introduces “typically” wetter conditions.

Interestingly, the groupings of positive rainfall departures tend to follow, rather than coincide with, La Niña episodes in PNG (Fig. 7). Furthermore, landslide-triggering events tend to coincide with La Niña episodes or ENSO neutral episodes and are less directly coincident to the groupings of positive rainfall departures. El Niño episodes tend to coincide with seasons where none or very few landslide-triggering events occur and where large negative departures from the 6-monthly mean rainfall are observed. These departures are usually greatest in the drier season. However, landslide-triggering events continue to occur particularly during the wetter seasons of El Niño episodes (i.e. 1987 and 1992; Fig. 7). This can partially be explained by reviewing the variability of the wetter season RAI to the drier season RAI. Figure 8 shows that 6-monthly rainfall exhibits larger variability between consecutive drier seasons, compared to variability between consecutive wetter seasons. The occurrence of El Niño and La Niña events appears to have a large influence on the drier season rainfall variability, as the peaks and troughs in the drier season 3 year running mean illustrate, but limited influence on the wetter season RAI. Therefore landslide-triggering events continue to occur during the north-westerly monsoon season during all phases of ENSO, but less landslide-triggering events are observed during drier season months during El Niño phases, than either La Niña or ENSO neutral periods.

Landslide inventory development in a data sparse region

J. C. Robbins and
M. G. Petterson

[Title Page](#)[Abstract](#)[Introduction](#)[Conclusions](#)[References](#)[Tables](#)[Figures](#)[⏪](#)[⏩](#)[◀](#)[▶](#)[Back](#)[Close](#)[Full Screen / Esc](#)[Printer-friendly Version](#)[Interactive Discussion](#)

3.3 Spatial characteristics of landslide occurrence

As with the temporal variability, landslide-triggering events are very unevenly distributed spatially across PNG (Fig. 9a). Higher densities of landslide occurrences are observed in provinces which intersect the mountainous central spine of the country. The highest densities are seen in Western Highlands, Chimbu, Western, Central and West Sepik Provinces as well as in the Huon Peninsula in Morobe Province. The spatial distribution of the landslide entries appears to be determined primarily by a combination of relief, precipitation and population density. The high density pocket of landslide activity observed in northern Western Province coincides with the area of greatest annual rainfall (Fig. 9b). This zone of high rainfall accumulations extends towards the south-east as a band, following the southern edge of the Papuan Fold Belt. The area directly south of the Fold Belt, where the highest rainfall accumulations tend to be observed, is comprised of predominantly flat, swampy plains and therefore records of landslide activity are scarce in these areas. The northern edge of this band of high rainfall accumulations coincides with relief which exceeds 1000 m and this is where clusters of landslides begin to be observed, extending down the southern edge of the Papuan Fold belt in parallel with the band of high annual rainfall accumulations.

Additional high density pockets of landslide occurrence are seen in Western Highlands and Chimbu Provinces (Fig. 9a), which lie within the central mainland cordillera where annual rainfall totals exceed 2700 mm yr^{-1} and relief can exceed 3000 m in places. The terrain is very rugged and slope angles can vary significantly, up to 50° . Despite this, these areas are some of the most densely populated of the mountainous-rural provinces in PNG, increasing the likelihood for landslides to interact with communities and infrastructure and be recorded (Fig. 9c). In addition, these areas also have high percentages of total cultivated land areas compared to their total land area, with Western Highlands, Chimbu and Eastern Highlands Provinces having 50, 42 and 50 % total cultivated land areas, respectively (Saunders, 1993; Bourke and Harwood, 2009). This compares to the southern Provinces (Western, Gulf, National Capital District and

Landslide inventory development in a data sparse region

J. C. Robbins and
M. G. Petterson

[Title Page](#)

[Abstract](#)

[Introduction](#)

[Conclusions](#)

[References](#)

[Tables](#)

[Figures](#)



[Back](#)

[Close](#)

[Full Screen / Esc](#)

[Printer-friendly Version](#)

[Interactive Discussion](#)



events are broadly confined to the central mainland cordillera and mountainous areas (north-west Toricelli Mountains and north-central Adelbert Range during DJF and south-east Owen Stanley Range on the Papuan Peninsula during SON) of the country.

Of the four seasons, the greatest spatial spread of landslide occurrences tends to occur during JJA and MMA (Fig. 10). The reasons for this are different in each case. As identified in Fig. 6, landslide-triggering events during JJA tend to be associated with exceptional rainfall which exceeds the 80th percentile for the month of initiation. Rainfall during this season is driven predominantly by orographic and physiographically-induced processes. These mesoscale features, including mesoscale convective complexes, mountain-valley winds and land-sea breezes, lead to localised, smaller-scale rainfall events affecting distinct regions of PNG (i.e. southern coast of New Britain and the north-eastern mainland region of the Huon Peninsula). The exception to this is the area in northern-Western Province, close to the border with Indonesia, which maintains moderate-to-high rainfall totals throughout the year. The dynamical processes driving rainfall appear to broadly coincide with locations which experience landslide activity at this time of year and in fact rainfall can be considered the dominant process affecting the spatial variability of landslides during this season. However, while it is possible to identify potential zones where mesoscale features may induce rainfall more regularly and by extension trigger landslides during this season, identifying actual locations of landslides cannot be determined due to the large degrees of variability inherent to this season. By comparison the large spread of landslide-triggering events across PNG during MAM is associated with the widespread dominance of deep convection induced by the north-westerly monsoon. Both the central cordillera and areas of lower elevation are affected by landsliding, during the wetter season, due to the increase in water availability and the interaction of this water with a larger number of potentially susceptible slopes. During MAM therefore, rainfall is the less dominant process determining the spatial variability of landsliding, as the vast majority of the region experiences high rainfall accumulations during this time. It is likely therefore, that underlying landslide

Landslide inventory development in a data sparse region

J. C. Robbins and
M. G. Petterson

[Title Page](#)

[Abstract](#)

[Introduction](#)

[Conclusions](#)

[References](#)

[Tables](#)

[Figures](#)

[⏪](#)

[⏩](#)

[◀](#)

[▶](#)

[Back](#)

[Close](#)

[Full Screen / Esc](#)

[Printer-friendly Version](#)

[Interactive Discussion](#)



are generally better documented. This is largely due to landslides being categorized as secondary hazards to earthquakes or flooding which are the primary hazards. In such cases the spatial and temporal information related to landslides is very poor.

As noted in Sect. 2.1 the timing of many landslides is uncertain, particularly where there are no eye witness accounts to the event. To capture this uncertainty and constrain the landslide event for comparison with rainfall climatology data, the time of initiation was approximated using a minimum and maximum date boundary relating to the earliest and latest dates within which the landslide event occurred. These dates generally relate to the start and end dates of potential landslide-triggering events, such as a flood event. Landslides were then grouped by month (Figs. 5 and 6) or season (Figs. 7 and 10) using the end date information. This has the potential to introduce errors where landslides are assigned to a month or season which does not correspond to its time of actual initiation. In turn, this could mean that a landslide-triggering event is not being compared against the correct rainfall climatology data and that patterns of activity associated with a specific season may be over or under-represented based on the bias introduced by using this metric. Although this cannot be ruled out completely, it has been possible to determine that 80% of all landslide entries in the database are constrained within a 10 day period or less. This means that the vast majority of landslides were initiated over a defined 10 day (or less) period and therefore we can be confident that these events are assigned to the correct 3- or 6-monthly season in the majority of cases. There is slightly more uncertainty for events assigned to monthly timescales, as where 10 day periods cross from one month into the next, the latest month will always be used. Towards the end of the wetter season, the numbers of flood-associated trigger mechanisms tends to increase and the number of days between the minimum and a maximum date boundaries also tends to increase. We believe that this helps to explain the second peak in rainfall-associated, landslide-triggering events observed in May (Fig. 5), which is more traditionally seen as a period of transition as the north-westerly monsoon period wanes and the south-easterly trade flows become more dominant.

Landslide inventory development in a data sparse region

J. C. Robbins and
M. G. Petterson

[Title Page](#)

[Abstract](#)

[Introduction](#)

[Conclusions](#)

[References](#)

[Tables](#)

[Figures](#)

[⏪](#)

[⏩](#)

[◀](#)

[▶](#)

[Back](#)

[Close](#)

[Full Screen / Esc](#)

[Printer-friendly Version](#)

[Interactive Discussion](#)



Landslide inventory development in a data sparse region

J. C. Robbins and
M. G. Petterson

[Title Page](#)[Abstract](#)[Introduction](#)[Conclusions](#)[References](#)[Tables](#)[Figures](#)[Back](#)[Close](#)[Full Screen / Esc](#)[Printer-friendly Version](#)[Interactive Discussion](#)

In spite of the limitations described above, we believe that this new, national-scale landslide inventory accurately captures those high-impact landslides which contribute to the majority of landslide fatalities and damage. As these are the types of landslide events which we would ideally like to mitigate against in the future, understanding how, when and where these events occur across space and time is very valuable. The findings illustrate that these landslides are strongly controlled by the annual north-westerly monsoon cycle and that during different phases of the seasonal cycle landslides are potentially triggered by very different magnitudes of rainfall (Fig. 6). Future research would hope to assess the long term trends in landslide activity at a regional-scale and assess how these changes are linked to changes in the climate, the strength of the monsoon cycle and ENSO. In order to do this effectively, continued development of the database and a more systematic approach to landslide recording is essential, so that this type analysis can be extended.

5 Conclusion

Regional-scale landslide inventories offer a greater understanding of the temporal and spatial distribution of landslide events, their characteristics and triggers. In this study we have constructed the first, regional-scale landslide inventory for PNG, bringing together a range of existing and new datasets to form a single, commonly formatted database of landslide entries. Whilst the challenges involved in the development of the database have been described in detail, we believe that the database constitutes a significant advance in knowledge and data that can be used by researchers and planners alike. Analyses of the newly collated landslide inventory demonstrates how this information can be used to understand regional-scale, spatial and temporal variability and the relationships between landslides and different trigger factors. The key findings from this research are:

Landslide inventory development in a data sparse region

J. C. Robbins and
M. G. Petterson

Title Page	
Abstract	Introduction
Conclusions	References
Tables	Figures
⏪	⏩
◀	▶
Back	Close
Full Screen / Esc	
Printer-friendly Version	
Interactive Discussion	

- Rainfall and the various combinations of triggers associated with it, account for the majority (~ 61 %) of all medium to large landslide-triggering events in the PNG inventory.
- There is also a strong climatic control on the landslide-triggering events, with greater numbers being observed between December and March, with a second peak in May, and fewer observed between June and October. This relates closely to periods dominated by north-westerly monsoon flows and south-easterly trade flows respectively.
- The majority of landslides initiated in the drier season are linked to extreme rainfall (~ 61 %), while landslides initiated during the wetter season can be triggered during months with lower absolute rainfall totals.
- In addition, there is large year to year variability in the annual occurrence of landslide events and this can be linked to different phases of ENSO. Landslide-triggering events continue to occur throughout north-westerly monsoon seasons in all phases of ENSO, but fewer numbers are observed during drier season months of El Niño phases, than either La Niña or ENSO neutral phases.
- The spatial distribution of landslide-triggering events is primarily determined by a combination of relief, precipitation and population density.

The information collected and analysed in this study contributes to the first country-wide assessment of landslides which result in fatalities and significant damage. Based on this analysis, landslide hazard hotspots and relationships between landslide occurrence and rainfall climatology can be identified. This information can prove important and valuable in the assessment of trends and future behaviour, which can be useful for policy makers and planners.



Acknowledgements. This research was jointly supported by the Met Office, University of Leicester and the University of Papua New Guinea. Special thanks go to colleagues at the PNG Mineral Resources Authority (MRA) and the Department of Mineral Policy and Geohazards Management in Papua New Guinea for their help and support throughout the completion of this research.

References

- Adler, R. F., Huffman, G. J., Chang, A., Ferraro, R., Ping-Ping Xie, Janowiak, J., Rudolf, B., Schneider, U., Curtis, S., Bolvin, D., Gruber, A., Susskind, J., Arkin, P. And Nelkin, E.: The Version 2 Global Precipitation Climatology Project (GPCP) monthly precipitation analysis (1979–present), *J. Hydrometeorol.*, 6, 1147–1167, 2003.
- Anton, L. and Gibson, G.: Analysing earthquake hazard in Papua New Guinea, in: Proceedings of the Australia Earthquake Engineering Society Conference, Ballarat, Australia, available at: <http://www.aees.org.au/wp-content/uploads/2013/11/14-Anton.pdf> (last access: 6 August 2015), 2008.
- Blong, R. J.: Mudslides in the Papua New Guinea Highlands, in: Proceedings of the 4th International Conference and Field Workshop on Landslides, Tokyo, Japan, 1985.
- Blong, R. J.: Natural hazards in the Papua New Guinea highlands, *Mt. Res. Dev.*, 6, 233–246, 1986.
- Bourke, R. M. and Harwood, T. (Eds): Food and Agriculture in Papua New Guinea, ANU E Press, The Australian National University, Canberra, Australia, 38–45, 2009.
- Brakenridge, G. R.: Global Active Archive of Large Flood Events, Dartmouth Flood Observatory, University of Colorado, available at: <http://floodobservatory.colorado.edu/Archives/index.html> (last access: 8 July 2015), 2010.
- Brakenridge, G. R. and Karnes, D.: The Dartmouth Flood Observatory: an electronic research tool and electronic archive for investigations of extreme flood events, Geological Society of 25 America Annual Meeting, Geoscience Information Society Proceedings, Denver, USA, 1996.
- Center for International Earth Science Information Network – CIESIN – Columbia University, International Food Policy Research Institute – IFPRI, The World Bank, and Centro Inter-
- nacional de Agricultura Tropical – CIAT, Global Rural-Urban Mapping Project, Version 1

Landslide inventory development in a data sparse region

J. C. Robbins and
M. G. Petterson

Title Page

Abstract

Introduction

Conclusions

References

Tables

Figures

⏪

⏩

◀

▶

Back

Close

Full Screen / Esc

Printer-friendly Version

Interactive Discussion



Landslide inventory development in a data sparse region

J. C. Robbins and
M. G. Petterson

[Title Page](#)

[Abstract](#)

[Introduction](#)

[Conclusions](#)

[References](#)

[Tables](#)

[Figures](#)



[Back](#)

[Close](#)

[Full Screen / Esc](#)

[Printer-friendly Version](#)

[Interactive Discussion](#)



(GRUMPv1): Population Density Grid, NASA Socioeconomic Data and Applications Center (SEDAC), Palisades, NY, doi:10.7927/H4R20Z93, 2011.

Comegna, L., Picarelli, L., and Urciuoli, G.: The mechanics of mudslides as a cyclic undrained-drained process, *Landslides*, 4, 271–232, 2007.

5 EM-DAT: The OFDA/CRED International Disaster Database, Université Catholique de Louvain, Brussels, Belgium, available at: <http://www.em-dat.net>, last access: 14 May 2015.

Greenbaum, D., Tutton, M., Bowker, M. R., Browne, T. J., Grealley, K. B., Kuna, G., McDonald, A. J. W., Marsh, S. H., Northmore, K. J., O'Connor, E. A., and Tragheim, D. G.: Rapid methods of landslide hazard mapping: Papua New Guinea case study, British Geological Survey

10 Technical Report WC/95/27, British Geological Survey, Nottingham, UK, 1995.

Guha-Sapir, D. and Below, R.: The quality and accuracy of disaster data – a comparative analysis of three global data sets, Working paper prepared for the Disaster Management Facility, World Bank, CRED, Brussels, available at: www.cred.be/sites/default/files/Quality_accuracy_disaster_data.pdf (last access: 14 May 2015), 2002.

15 Guzzetti, F., Peruccacci, S., Rossi, M., and Stark, C. P.: Rainfall thresholds for the initiation of landslides in central and southern Europe, *Meteorol. Atmos. Phys.*, 98, 239–267, 2007.

Hill, K. C. and Hall, R.: Mesozoic-Cenozoic evolution of Australia's New Guinea margin in a west Pacific context, in: *Defining Australia: The Australian Plate*, edited by: Hillis, R. and Müller, R. D., *Geol. Soc. Australia Spec. Pub. 22 and GSA Spec. Paper 372*, Geological Society of

20 America, Boulder, Colorado, 259–283, 2003.

Hovius, N., Stark, C. P., Tutton, M. A., and Abbott, L. D.: Landslide-driven drainage network evolution in a pre-steady-state mountain belt: Finisterre Mountains, Papua New Guinea, *Geology*, 26, 1071–1074, 1998.

Iverson, R. M.: Landslide triggering by rain infiltration, *Water Resour. Res.*, 36, 1897–1910,

25 2000.

Keefer, D. K.: Investigating landslides caused by earthquakes – a historical review, *Surv. Geophys.*, 23, 473–510, 2002.

King, J. and Loveday, I.: Preliminary geological report on the effects of the earthquake of 11th May 1985 centred near Biallo, West New Britain, Geological Survey of Papua New Guinea Report 85/12, Geological Survey of Papua New Guinea, Port Moresby, 1985.

30 Kirschbaum, D. B., Adler, R., Hong, Y., and Lerner-Lam, A.: Evaluation of a preliminary satellite-based landslide hazard algorithm using global landslide inventories, *Nat. Hazards Earth Syst. Sci.*, 9, 673–686, doi:10.5194/nhess-9-673-2009, 2009.

Landslide inventory development in a data sparse region

J. C. Robbins and
M. G. Petterson

[Title Page](#)

[Abstract](#)

[Introduction](#)

[Conclusions](#)

[References](#)

[Tables](#)

[Figures](#)

[⏪](#)

[⏩](#)

[◀](#)

[▶](#)

[Back](#)

[Close](#)

[Full Screen / Esc](#)

[Printer-friendly Version](#)

[Interactive Discussion](#)



- Kirschbaum, D. B., Adler, R., Hong, Y., Hill, S., and Lerner-Lam, A.: A global landslide catalog for hazard applications: methods, results and limitations, *Nat. Hazards*, 52, 561–575, 2010.
- Kuna, G.: The impact of landslides on national highways in the Highlands Region, Papua New Guinea Geological Survey Technical Note TN 8/98, Port Moresby, Papua New Guinea, 1998.
- 5 McAlpine, J. R., Keig, G., and Falls, R.: Climate of Papua New Guinea, Commonwealth Scientific and Industrial Research Organization, Canberra, Australia, 1983.
- McGregor, G. R.: An assessment of the annual variability of rainfall: Port Moresby, Papua New Guinea, *Singapore, J. Trop. Geogr.*, 10, 43–54, 1989.
- 10 McGregor, G. R. and Nieuwolt, S.: Tropical Climatology, An Introduction to the Climates of the Low Latitudes, 2nd Edn., Wiley and Sons, Chichester, 1998.
- Meunier, P., Hovius, N., and Haines, A. J.: Regional patterns of earthquake-triggered landslide and their relation to ground motion, *Geophys. Res. Lett.*, 34, L20408, doi:10.1029/2007GL031337, 2007.
- Ota, Y., Chappell, J., Beryyman, K., and Okamoto, Y.: Late quaternary paleolandslides on the coral terraces of Huon Peninsula, Papua New Guinea, *Geomorphology*, 19, 55–76, 1997.
- Pain, C. F. and Bowler, J. M.: Denudation following the November 1970 earthquake at Madang, Papua New Guinea, *Z. Geomorphol., Suppl. Bd.*, 18, 92–104, 1973.
- Peart, M.: The Kaiapit Landslide: events and mechanisms, *Q. J. Eng. Geol. Hydrogeol.*, 24, 399–411, 1991a.
- 20 Peart, M.: Ok Tedi mining project: site visit 29 April to 2 May 1991, Papua New Guinea Geological Survey Technical Note TN 12/91, Port Moresby, Papua New Guinea, 1991b.
- Peart, M.: The geology and geotechnical properties of Chim Formation mudstones of Papua New Guinea, Papua New Guinea Geological Survey Technical Report 4/91, Papua New Guinea Geological Survey, Port Moresby, Papua New Guinea, 1991c.
- 25 Petley, D., Crick, W. O., and Hart, A. B.: The use of satellite imagery in landslide studies in high mountain areas, in: Proceedings of the Asian Conference on Remote Sensing, Kathmandu, Nepal, available at: <http://a-a-r-s.org/aars/proceeding/ACRS2002/Papers/HMD02-9.pdf> (last access: 6 August 2015), 2002.
- Petley, D., Hearn, G. J., Hart, A., Rosser, N. J., Dunning, S. A., Oven, K., and Mitchell, W. A.: Trends in landslide occurrence in Nepal, *Nat. Hazards*, 43, 23–44, 2007.
- 30 Petley, D.: Global patterns of loss of life from landslides, *Geology*, 40, 927–930, 2012.
- Qian, J.-H.: Why precipitation is mostly concentrated over islands in the maritime continent, *J. Atmos. Sci.*, 65, 1428–1444, 2008.

Table 1. Critical and relevant information obtained for each landslide entry in the new PNG landslide inventory.

Critical information collected in the database:	
Date	day.month.year/month.year
Location	Village, town or landmark
Province	Administrative province name
Relevant information collected in the database:	
Landslide Triggering Event (LTE) start date	Day Month Year
Landslide Triggering Event (LTE) end date	Day Month Year
LTE Duration in days	
Colloquial landslide name	
River/Catchment	
Landslide or landslide cluster location coordinates	X – Lat Y – Long
Number of landslides	
Landslide cluster group	0–10 10–100 100–1000 > 1000
Landslide type	
Landslide volume (combined or single landslide)	
Landslide affected area (combined or single landslide)	
Trigger/Event Descriptor	
Earthquake Date	day.month.year
Earthquake coordinates	X – Lat Y – Long
Earthquake Magnitude	
Earthquake Depth (km)	
Impacts of the landslide/landslide cluster	
Scientific/journal publication reference	
PNG MRA or DMPGM report reference	
Disaster Identifier reference (GLIDE, EM-DAT disaster No.)	
Media reference	
Humanitarian response reference	

Landslide inventory development in a data sparse region

J. C. Robbins and
M. G. Petterson

[Title Page](#)

[Abstract](#)

[Introduction](#)

[Conclusions](#)

[References](#)

[Tables](#)

[Figures](#)

[⏪](#)

[⏩](#)

[◀](#)

[▶](#)

[Back](#)

[Close](#)

[Full Screen / Esc](#)

[Printer-friendly Version](#)

[Interactive Discussion](#)



Landslide inventory development in a data sparse region

J. C. Robbins and
M. G. Petterson

[Title Page](#)

[Abstract](#)

[Introduction](#)

[Conclusions](#)

[References](#)

[Tables](#)

[Figures](#)



[Back](#)

[Close](#)

[Full Screen / Esc](#)

[Printer-friendly Version](#)

[Interactive Discussion](#)



Table 2. Typical DN value ranges, for each wavelength, indicative of active landslides (Petley, 2002).

Band number	Wavelength (micrometers)	DN values of active landslides
1	0.45–0.515	60–100
2	0.525–0.605	60–100
3	0.63–0.69	50–120
4	0.75–0.90	70–130
5	1.55–1.75	80–140
6	10.40–12.5	140–190
7	2.09–2.35	60–110

Landslide inventory development in a data sparse region

J. C. Robbins and
M. G. Petterson

[Title Page](#)

[Abstract](#)

[Introduction](#)

[Conclusions](#)

[References](#)

[Tables](#)

[Figures](#)

[⏪](#)

[⏩](#)

[◀](#)

[▶](#)

[Back](#)

[Close](#)

[Full Screen / Esc](#)

[Printer-friendly Version](#)

[Interactive Discussion](#)



Table 3. Return period in years for magnitude 6.0 earthquakes for selected tectonic seismic zones in PNG (Ripper and Letz, 1993).

Seismic zone	Seismic zone area (km ²)	Return period (yr) for magnitude 6.0 earthquake
Papuan Fold Belt	129 600	5.7
North Sepik	67 900	3.3
Ramu	86 400	1.9
Huon	40 100	1.9
New Britain	92 600	0.4
Bougainville Island	104 900	0.4

Landslide inventory development in a data sparse region

J. C. Robbins and
M. G. Petterson

[Title Page](#)

[Abstract](#)

[Introduction](#)

[Conclusions](#)

[References](#)

[Tables](#)

[Figures](#)



[Back](#)

[Close](#)

[Full Screen / Esc](#)

[Printer-friendly Version](#)

[Interactive Discussion](#)



Table 4. La Nina and El Nino years identified from bimonthly MEI ranks (based on data sourced in 2012).

La Niña years	El Niño years
1970–1971	1972–1973
1973–1976	1982–1983
1988–1989	1986–1987
1999–2001	1991–1992
2007–2009	1994–1995
	1997–1998

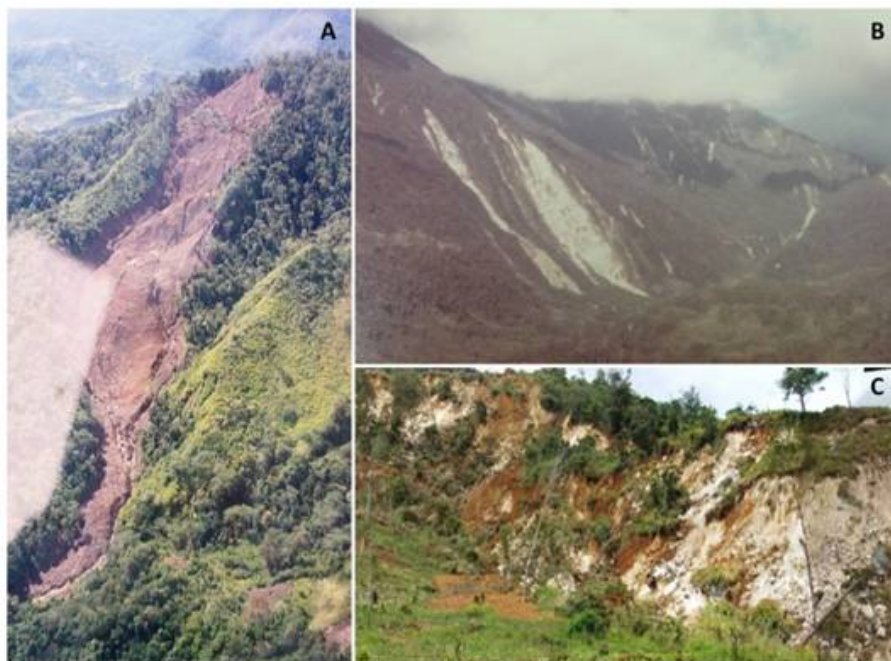


Figure 2. Photographs of landslides which have occurred in PNG: **(a)** debris flow near Dakgaman Village, Morobe Province; **(b)** Bolovip Mission, Western Province; **(c)** back-scarp of a rotational soil slump at Gera village, Chimbu Province. Photographs courtesy of the MRA.

Landslide inventory development in a data sparse region

J. C. Robbins and
M. G. Petterson

[Title Page](#)

[Abstract](#)

[Introduction](#)

[Conclusions](#)

[References](#)

[Tables](#)

[Figures](#)

[⏪](#)

[⏩](#)

[◀](#)

[▶](#)

[Back](#)

[Close](#)

[Full Screen / Esc](#)

[Printer-friendly Version](#)

[Interactive Discussion](#)



Landslide inventory development in a data sparse region

J. C. Robbins and
M. G. Petterson

[Title Page](#)

[Abstract](#)

[Introduction](#)

[Conclusions](#)

[References](#)

[Tables](#)

[Figures](#)

[⏪](#)

[⏩](#)

[◀](#)

[▶](#)

[Back](#)

[Close](#)

[Full Screen / Esc](#)

[Printer-friendly Version](#)

[Interactive Discussion](#)

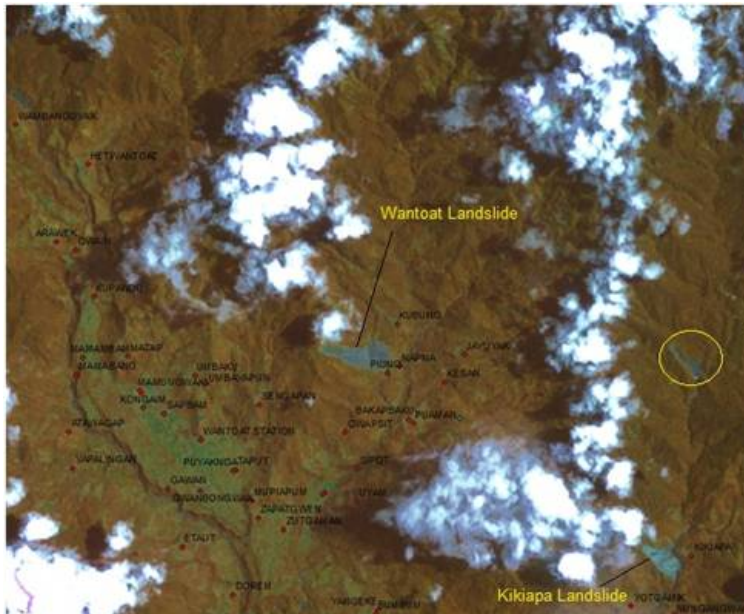


Figure 3. FCC 457 ETM+ image, acquired on 21 September 2002, showing the Wantoat, Kikiapa and Dakgaman (circled) landslides.

Landslide inventory development in a data sparse region

J. C. Robbins and
M. G. Petterson

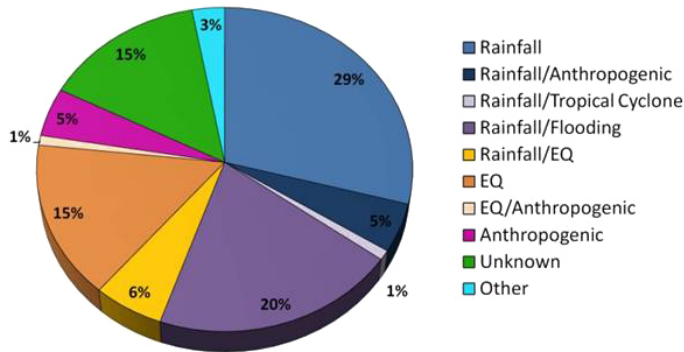


Figure 4. Distribution of landslide-triggering event types associated with landslides and landslide clusters recorded in the PNG landslide inventory between 1970 and 2013.

[Title Page](#)

[Abstract](#) | [Introduction](#)

[Conclusions](#) | [References](#)

[Tables](#) | [Figures](#)

[⏪](#) | [⏩](#)

[◀](#) | [▶](#)

[Back](#) | [Close](#)

[Full Screen / Esc](#)

[Printer-friendly Version](#)

[Interactive Discussion](#)



Landslide inventory development in a data sparse region

J. C. Robbins and
M. G. Petterson

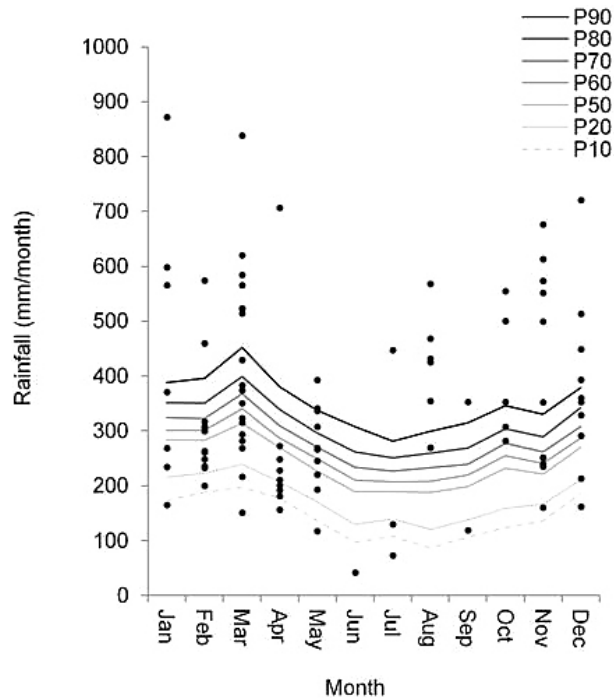


Figure 6. Percentiles of monthly precipitation calculated based on the 53 GPCC grid squares representing landslide affected areas in PNG (1970–2010) and landslide-triggering events.

[Title Page](#)

[Abstract](#)

[Introduction](#)

[Conclusions](#)

[References](#)

[Tables](#)

[Figures](#)



[Back](#)

[Close](#)

[Full Screen / Esc](#)

[Printer-friendly Version](#)

[Interactive Discussion](#)



Landslide inventory development in a data sparse region

J. C. Robbins and
M. G. Petterson

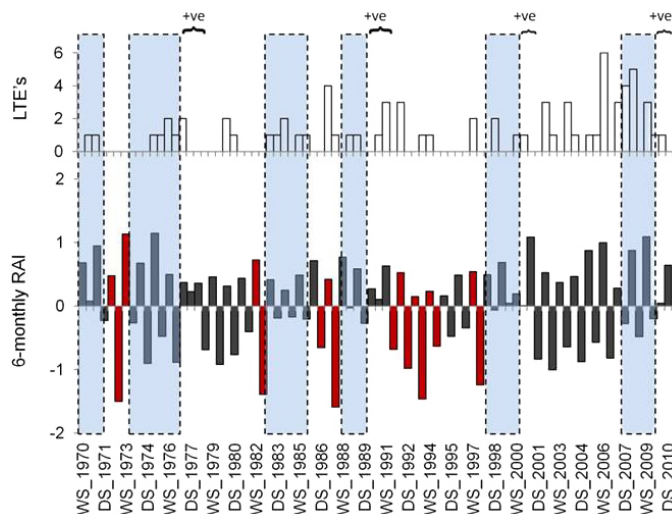


Figure 7. Bar charts show 6-monthly landslide-triggering events (white bars, top plot) and the corresponding 6-monthly rainfall anomaly index (grey bars, bottom plot). La Niña episodes are shown by the shaded blue columns, while consecutive 6-monthly periods with positive departures from the mean are identified by the “+ve” labels. Seasons associated with El Niño are shown by the red bars.

[Title Page](#)

[Abstract](#)

[Introduction](#)

[Conclusions](#)

[References](#)

[Tables](#)

[Figures](#)



[Back](#)

[Close](#)

[Full Screen / Esc](#)

[Printer-friendly Version](#)

[Interactive Discussion](#)



Landslide inventory development in a data sparse region

J. C. Robbins and
M. G. Petterson

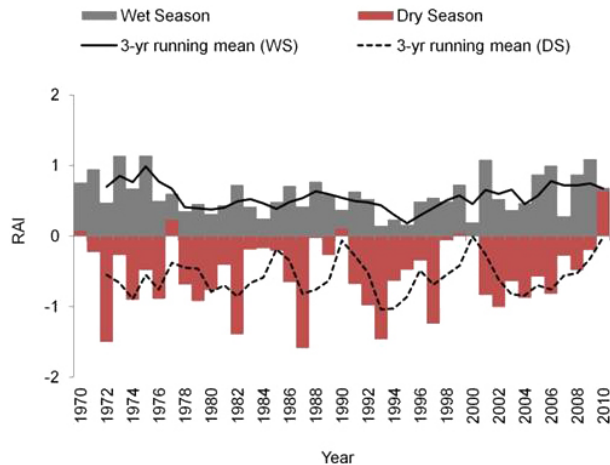


Figure 8. Comparison between wet season 6-monthly rainfall anomaly index and dry season 6-monthly rainfall anomaly index.

[Title Page](#)[Abstract](#)[Introduction](#)[Conclusions](#)[References](#)[Tables](#)[Figures](#)[⏪](#)[⏩](#)[◀](#)[▶](#)[Back](#)[Close](#)[Full Screen / Esc](#)[Printer-friendly Version](#)[Interactive Discussion](#)

Landslide inventory development in a data sparse region

J. C. Robbins and
M. G. Petterson

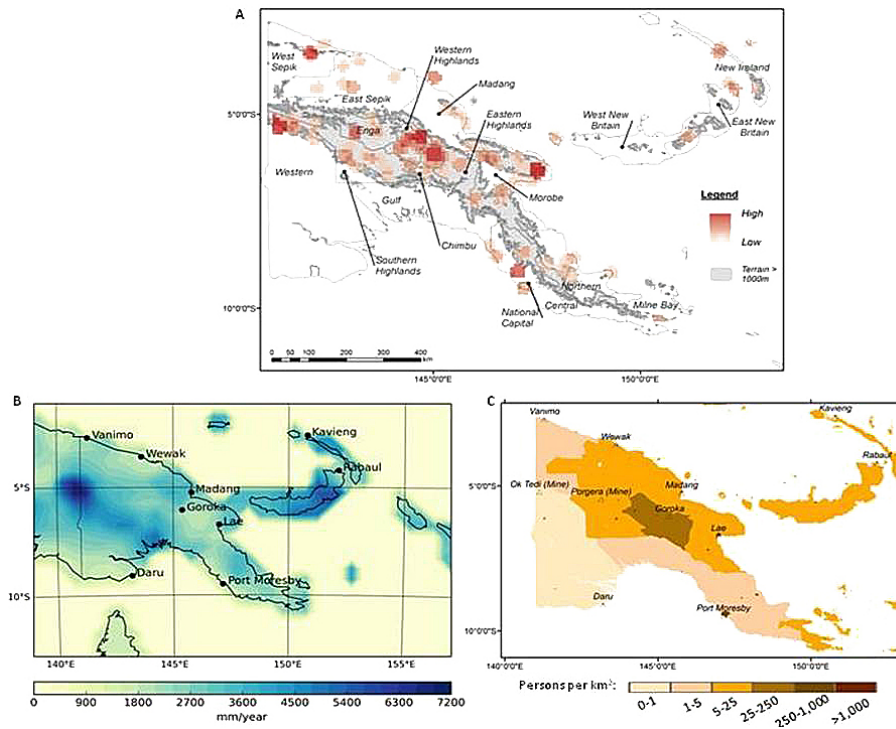


Figure 9. (a) The distribution of landslide entries between 1970 and 2013 shown as the density of latitude/longitude points around each 10 km² cell using a neighbourhood radius of 30 km. (b) The corresponding distribution of mean annual precipitation calculated over the period 1970 to 2010. (c) Population density measured as the number of persons per square kilometre of land area with a grid resolution of 30 arcsec (data produced by the Global Rural-Urban Mapping Project (GRUMPv1) and made available by the Center for International Earth Science Information Network (CIESIN)).

Landslide inventory development in a data sparse region

J. C. Robbins and
M. G. Petterson

[Title Page](#)

[Abstract](#)

[Introduction](#)

[Conclusions](#)

[References](#)

[Tables](#)

[Figures](#)

[⏪](#)

[⏩](#)

[⏴](#)

[⏵](#)

[Back](#)

[Close](#)

[Full Screen / Esc](#)

[Printer-friendly Version](#)

[Interactive Discussion](#)

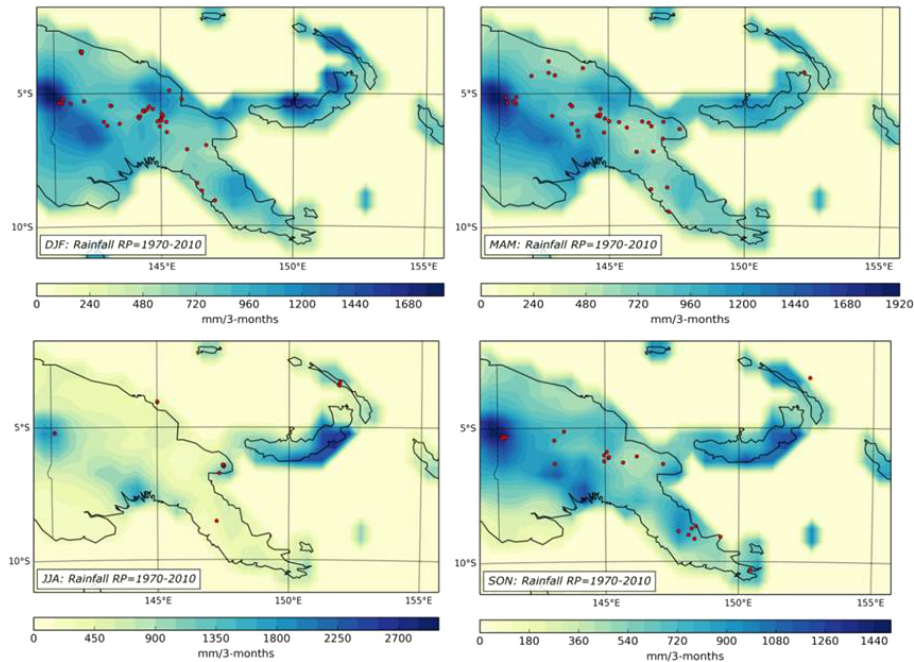


Figure 10. Seasonal composites of 3-monthly rainfall based on the 41 year reference period (RP) with all landslide entries linked to rainfall trigger mechanisms (1970–2013) overlain and shown by season using red dots.

Landslide inventory development in a data sparse region

J. C. Robbins and M. G. Petterson

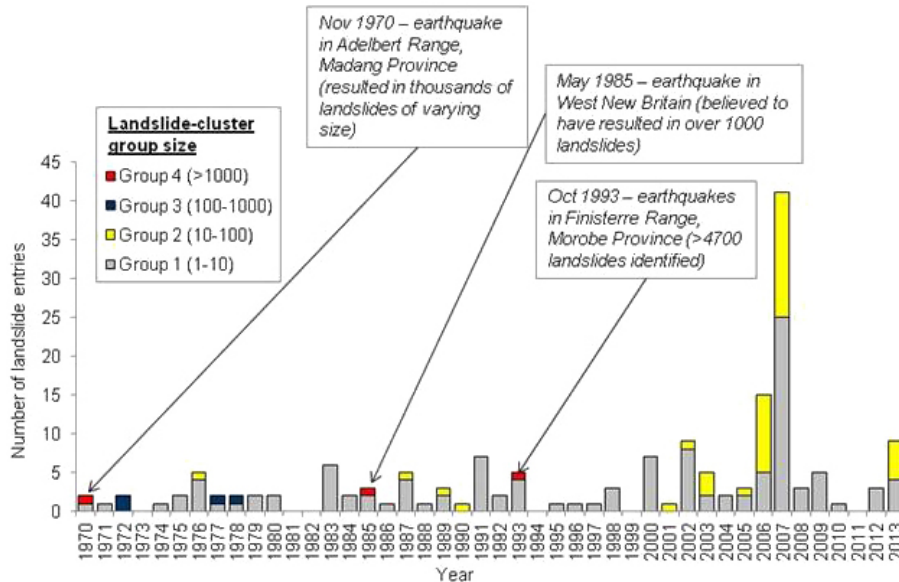


Figure 11. Landslide entries in the PNG landslide inventory showing the temporal distribution of events and the uncertainty in total numbers of landslides associated with each entry.

[Title Page](#)

[Abstract](#) | [Introduction](#)

[Conclusions](#) | [References](#)

[Tables](#) | [Figures](#)

[⏪](#) | [⏩](#)

[◀](#) | [▶](#)

[Back](#) | [Close](#)

[Full Screen / Esc](#)

[Printer-friendly Version](#)

[Interactive Discussion](#)

